

# Intermittency and Synchronisation in Gumowski-Mira Maps

G. Ambika and K. Ambika

*Department of Physics, Maharaja's College, Cochin-682011, India.*

---

## Abstract

The Gumowski-Mira map is a 2-dimensional recurrence relation that provide a large variety of phase space plots resembling fractal patterns of nature. We investigate the nature of the dynamical states that produce these patterns and find that they correspond to Type I intermittency near periodic cycles. By coupling two GM maps, such patterns can be wiped out to give synchronised periodic states of lower order. The efficiency of the coupling scheme is established by analysing the error function dynamics.

*Key words:* chaos, Gumowski-Mira map, bifurcation, synchronisation.

---

## 1 Introduction

Non linear recurrence relations model many real world systems and help in analysing their possible asymptotic behaviour as the parameters are varied [1]. Here we analyse one such recurrence map defined through a 2-dimensional difference equation called Gumowski-Mira transformation [2]. This system involves a non linear function  $f(x)$  that is advanced in time by one iteration, in the  $y$  equation. It has been reported that computer simulations of this iterative scheme [3] give rise to a variety of 2-dimensional images in the phase plane  $(x, y)$  called GM patterns that resemble natural objects like star fish, jelly fish, wings of a butterfly, sections of fruits, flowers of varying shapes etc. Apart from a mere fascination in creating these patterns, one can implement a scheme like Iterative function scheme for producing 2-dimensional fractals or fractal objects of nature using this map for different values of the parameters involved. Moreover, the final pattern is found to depend very sensitively on the

---

*Email address:* ambika@iucaa.ernet.in (G. Ambika).

parameters, a feature which can be exploited in decision making algorithms and control techniques in computing and communication.

One motivation in this work is to analyse the underlying dynamics behind the formation of these patterns and their possible bifurcation sequences. In this context, we would like to mention that the period doubling sequences and chaos doubling phenomenon in this system has been reported earlier for a chosen set of parameter values [4]. We are concentrating on another set that was used in [3] for generating GM patterns. Here the dynamics involved is different in the sense that the intermittency route and odd period cycles predominate and the route to chaos is via formation of quasiperiodic bands and band mergings. The detailed evolution of the basin structure during the scenario until onset of chaos and final escape forms part of our work. The scaling behaviour near intermittency, stability of the lowest periodic cycles are also analysed. Moreover our work provides evidence for periodic window and repeated substructures in the bifurcation scenario which show self similarity with respect to scaling in the parameter. This can therefore account for the sensitive dependence of the asymptotic dynamical states or phase portraits on the relevant parameter of the system.

It has been reported that [5] the lowest order periodic orbits of the GM map are non parametric in nature and hence a straight forward application of OGY scheme to control chaos in the system is not desirable. Hence this is achieved through a proxy system in [5]. We introduce a simple and straight forward linear and mutual coupling scheme to achieve the same result. Moreover by coupling two such maps synchronised states with low periodic cycles can be produced. Periodicity with synchronicity is found to be quite robust in the system even against considerable perturbations. A detailed analysis of the error function dynamics is carried out to estimate the average synchronisation time  $\langle \tau_1 \rangle$  and the stabilisation time  $\langle \tau_2 \rangle$  after a perturbation is applied.

In this paper, Section 2 introduces the GM map and its possible stable dynamical states. Section 3 gives the results of a detailed numerical analysis of the predominant bifurcation sequences in the map. The intermittency and other routes to chaos are given in Section 4. In Section 5, the control of chaos and synchronisation of the coupled maps is discussed. The discussion of the main results are given in Section 6.

## 2 Dynamical States of GM map.

The transformation of Gumowski-Mira map that has been studied in computer simulations can be written as a 2-dimensional recurrence relation defined in the  $x - y$  plane as

$$\begin{aligned}
x_{n+1} &= y_n + a(1 - by_n^2)y_n + f(x_n) \\
y_{n+1} &= -x_n + f(x_{n+1})
\end{aligned} \tag{1}$$

with  $f(x_n) = \mu x_n + \frac{2(1-\mu)}{1+x_n^2}x_n^2$ . It should be noted that the function  $f(x)$  in the  $y$  equation is advanced in time by one iteration which provides richer and complex dynamical behaviour. The nature of variation of the non linear function  $f(x_0)$  as well as  $f(x_1)$  for different  $\mu$  values in the range  $-0.3$  to  $+0.0039$  with  $a = 0.008$  and  $b = 0.05$  is shown in figs 1a and 1b. Here  $x_0$  is the starting seed value and  $x_1$  is the first iterate. These figures give an indication of how different the functions in the  $x$  and  $y$  equations are and how fast and differently they change as iterations proceed. As any stable periodic cycle is reached asymptotically, these functions are found to level off.

The one cycle fixed points of the system is determined by solving the equations

$$\begin{aligned}
x &= y + a(1 - by^2)y + \mu x + \frac{2(1 - \mu)x^2}{1 + x^2} \\
y &= (\mu - 1)x + \frac{2(1 - \mu)x^2}{1 + x^2}
\end{aligned} \tag{2}$$

using MAXIMA and the only real and bounded solutions of interest are  $(0, 0)$  and  $(1, 0)$ , which are unstable in the relevant parameter regions of our study. The most prominent elementary cycle here is a 4 cycle born by saddle node bifurcation. The stability of this 4 cycle can be established numerically by calculating the eigen values of the Jacobian  $M$  for chosen values of  $\mu$  and the corresponding elements of the 4 cycle. Thus if  $(\delta x_n, \delta y_n)$  are the small perturbations to the cycle elements, we have

$$\begin{pmatrix} \delta x_{n+1} \\ \delta y_{n+1} \end{pmatrix} = M \begin{pmatrix} \delta x_n \\ \delta y_n \end{pmatrix}. \tag{3}$$

where

$$\begin{aligned}
M_{11} &= -\frac{4x^3(1-\mu)}{(1+x^2)^2} + \frac{4x(1-\mu)}{1+x^2} + \mu \\
M_{12} &= 1 - 2aby^2 + a(1 - by^2) \\
M_{21} &= -1 + \mu \left( -\frac{4x^3(1-\mu)}{(1+x^2)^2} + \frac{4x(1-\mu)}{1+x^2} + \mu \right) - \\
&\quad \frac{4(1-\mu) \left( -\frac{4x^3(1-\mu)}{(1+x^2)^2} + \frac{4x(1-\mu)}{1+x^2} + \mu \right) \left( y + ay(1 - by^2) + \frac{2x^2(1-\mu)}{1+x^2} + x\mu \right)^3}{\left( 1 + (y + ay(1 - by^2) + \frac{2x^2(1-\mu)}{1+x^2} + x\mu)^2 \right)^2} + \\
&\quad \frac{4(1-\mu) \left( -\frac{4x^3(1-\mu)}{(1+x^2)^2} + \frac{4x(1-\mu)}{1+x^2} + \mu \right) \left( y + ay(1 - by^2) + \frac{2x^2(1-\mu)}{1+x^2} + x\mu \right)}{1 + (y + ay(1 - by^2) + \frac{2x^2(1-\mu)}{1+x^2} + x\mu)^2}
\end{aligned} \tag{4}$$

$$\begin{aligned}
M_{22} &= (1 - 2aby^2 + a(1 - by^2))\mu - \\
&\quad \frac{4(1 - 2aby^2 + a(1 - by^2))(1 - \mu) \left( y + ay(1 - by^2) + \frac{2x^2(1-\mu)}{1+x^2} + x\mu \right)^3}{\left( 1 + (y + ay(1 - by^2) + \frac{2x^2(1-\mu)}{1+x^2} + x\mu)^2 \right)^2} + \\
&\quad \frac{4(1 - 2aby^2 + a(1 - by^2))(1 - \mu) \left( y + ay(1 - by^2) + \frac{2x^2(1-\mu)}{1+x^2} + x\mu \right)}{1 + (y + ay(1 - by^2) + \frac{2x^2(1-\mu)}{1+x^2} + x\mu)^2}
\end{aligned}$$

The eigen values of  $M$  evaluated for a few typical  $\mu$  values with  $a = 0.008$ ;  $b = 0.05$  in the 4 cycle window are given in 1 .

Table 1

The Eigen values of the stability matrix for different  $\mu$  values in the 4 cycle window  $|E| < 1$  in all the above cases indicating stability of the concerned 4 cycle [6]

$\mu$	$E_1$	$E_2$
-0.0964	0.6384	-0.6346
-0.095	0.6451	-0.6415
-0.005	0.9371	-0.9371
0.0002	0.8169	-0.8169
0.0003	0.7841	-0.7841

### 3 Bifurcation Sequence.

We have mentioned that the asymptotic dynamical states of the GM map depends sensitively on the parameter  $\mu$ . In this section, we numerically investigate in detail, the possible states and their bifurcation patterns as  $\mu$  is varied.

We find that the bounded interval for the map lies in the interval  $[-1, 1]$  for  $a = 0.008$  and  $b = 0.05$ . Moreover the most prominent elementary cycle of periodic behaviour is 4 which occurs in many intermittent windows of  $\mu$  in the bifurcation diagram. The full scenario is given in Fig 2a which is mostly dominated by broad windows of odd cycles like 7, 11 etc. Here out of 10,000 iterate 9000 are discarded as initial transients and the next 1000 are plotted. The specific regions of the windows of such cycles are zoomed and reproduced in Fig 2b, 2c and 2d.

In general these windows of periodic cycles born by tangent bifurcations or saddle node bifurcations at their left ends exhibit intermittency behaviour in their iterates. The transition to chaos takes place for small increase of values of  $\mu$  when the periodic cycle becomes unstable giving rise to quasiperiodic bands which become chaotic and merge together. We illustrate this for the 7 cycle window. Near the left end of a periodic 7 cycle window Fig 3a gives the  $x_n - n$  plot with  $\mu = -0.2734$  for 6000 iterations showing intermittently laminar and chaotic behaviour. Fig 3b gives the corresponding  $x - y$  plot. It is interesting to note that the periodic window structure shows self similarity in their substructures with respect to scaling in  $\mu$ . This is evident from the plots in Fig 3c and Fig 3d where a 7 cycle and a 22 cycle patterns repeat at two levels of zooming in the parameter range. This recurring self similarity with the consequent intermittency in the beginning of each periodic cycle and quasi-periodicity at its end, accounts for the variety and richness of the GM patterns in the  $x - y$  plane with its highly sensitive dependence on  $\mu$ .

#### 4 Intermittency & Transition to Chaos.

The nature of intermittency before the birth of a periodic cycle is analysed by calculating the average life time of the laminar region  $\langle l \rangle$  in the  $x_n - n$  plots. For one such region near  $\mu = -0.312501$  before a ten cycle window the variation of  $\langle l \rangle$  as a function of  $|\mu - \mu_c|$  is studied (Fig 4).  $\mu_c$  is the critical value when it becomes chaotic. We can write  $\langle l \rangle \sim |\mu - \mu_c|^\nu$ .  $\nu$  then defines the scaling index that helps to identify the type of intermittency. Here  $\mu_c = -0.312498$  and  $\nu = -0.49$  so that the intermittency is Type I [7] which is usually associated with saddle node bifurcation.

For further work we concentrate mainly on the stable window of the 4 cycle in the range  $-0.096 < \mu < 0.0003695$ .

The phase space during intermittency before the stabilisation of the 4 cycle, the 4 cycle region, the quasi periodic band region with 4 bands and final merging of bands to chaos are shown in Fig 5a–d. It is clear that the transition to chaos is via quasi-periodicity to chaotic bands and band merging. The

precise transition point is in this case  $\mu = 0.000369$ .

The evolution of the basin structure in the phase space during these transitions is also studied in detail and shown in Fig 6a–c.

The last figure 6d gives the basin boundary between bounded and escape regions, where escape takes place beyond  $\mu = +1$

## 5 Synchronisation and Control of Chaos.

We try a linear mutual coupling of two GM maps as a control mechanism, by which chaotic and intermittency regions can be targeted to stable low periodic regions.

The corresponding equations are

$$\begin{aligned}x1_{n+1} &= y1_n + a(1 - by1_n^2)y1_n + f(x1_n) + \varepsilon x2_n \\y1_{n+1} &= -x1_n + f(x1_{n+1}) \\x2_{n+1} &= y2_n + a(1 - by2_n^2)y2_n + f(x2_n) + \varepsilon x1_n \\y2_{n+1} &= -x2_n + f(x2_{n+1})\end{aligned}\tag{5}$$

where  $\varepsilon$  is the coupling parameter. We analyse this system numerically for  $\mu = -0.31$  and  $a = 0.008$ ,  $b = 0.05$ , both the maps individually exhibit chaotic behaviour. After coupling with  $\varepsilon = 1$  and initial values  $x1_0 = 0.1$ ,  $y1_0 = 0$  for the first map and  $x2_0 = 0.2$  and  $y2_0 = 0.1$  for the second map, both the maps are found to settle to 5 cycles. Here control of chaos and periodicity are achieved eventhough synchronisation is absent.

We are also able to synchronise two chaotic maps to lower periodicities using this coupling scheme. Eventhough much work is reported in the area of synchronisation [8], majority of these works are in continuous systems. However there are a few specific cases reported in the context of two dimensional map [9,10]. Here we achieve synchronisation in two coupled discrete maps of the GM type for  $\mu = -0.39$  with  $\epsilon = 0.7$ . Total synchronisation is seen in both  $x$  and  $y$  as the coupled system settles to identical 4 cycles. This is shown in Fig 7a.

The analysis is continued by developing the error function dynamics by defining the error in the  $x$  and  $y$  values of the two synchronising systems as  $e^x = (x1 - x2)$  and  $e^y = (y1 - y2)$ . Then their dynamics develops through the

following set of maps.

$$\begin{aligned}
e_{n+1}^x &= \left[ \mu + \frac{2(1-\mu)(x1_n + x2_n)}{(1+x1_n^2)(1+x2_n^2)} - \varepsilon \right] e_n^x \\
&\quad + \left[ 1 + a - ab(y1_n^2 + y1_n y2_n + y2_n^2) \right] e_n^y \\
e_{n+1}^y &= -e_n^x + \left[ \mu + \frac{2(1-\mu)(x1_{n+1} + x2_{n+1})}{(1+x1_{n+1}^2)(1+x2_{n+1}^2)} \right] e_{n+1}^x
\end{aligned} \tag{6}$$

The set of equations (5) and (6) are evolved together until  $e^x \rightarrow 0$  and  $e^y \rightarrow 0$  [11], when total synchronisation is said to be achieved.

From this the time for synchronisation is computed for 10 sets of initial values and the average is found to be  $\langle \tau_1 \rangle = 502$  for the typical values mentioned above.

The robustness of the mechanism is tested by applying a perturbation and the stabilisation time is calculated as the time to reach synchronisation again after it is disturbed. This is also repeated for 10 initial values and the average time  $\langle \tau_2 \rangle$  is found to be 473.

Fig 7b is the  $e^x - n$  plot showing  $\tau_1$  and  $\tau_2$  values for a perturbation of  $x_n = x_n + 10$  given after 2000 iterations. A similar plot is obtained for the error function in  $y$  also.

## 6 Conclusion

In this work we analyse the dynamics of the large variety of interesting and lively patterns exhibited by the GM map and find that they are attractors of the system in the phase plane in the neighbourhood of higher order cycles. The temporal behaviour then corresponds to intermittency of Type I with an exponent  $\sim -0.5$ .

The dependence of the phase space structure of the patterns on minute changes in the parameter makes it a useful tool in decision making algorithms. This sensitive dependence is due to the recurring periodic and self similar substructures in the bifurcation scenario, each with its own intermittency, periodicity, quasi periodic band and merging of bands leading to chaos. The nature and characterisation of these patterns and occurrence of crises related phenomena near them are being studied and will be reported else where.

The coupled states of these maps are either synchronised or they stabilise to attractors of the same periodicity, without amplitude synchronisation. A de-

tailed analysis of the error function dynamics is carried out to estimate average time for synchronisation and stabilisation time after applying a perturbation.

The relative efficiency of different schemes of coupling in synchronising 2 such maps to chosen dynamical states is intended as further study.

### *Acknowledgement*

We thank Prof. Y. Tanaka, College of Education, Ibaraki University, Mito, Japan for useful discussions through a private communication. One of us (G. Ambika) thank IUCAA, Pune for hospitality and computer facility.

### **References**

- [1] H. E. Nusse and J. A. Yorke, Dynamics - Numerical Exploitations.
- [2] Gumowski I. - Mira. C. (1980), Recurrence and Discrete Dynamic Systems, Springer.
- [3] K. Otsubo, M. Washida, T. Itoh, K. Katuara and M. Hayashi, Computer Simulations on the Gumowski-Mira Transformation. Forma 15.
- [4] M. Ali, L. M. Saha, Y. Tanaka and Hideo Soga, Bifurcation Scenario in Gumowski-Mira Map: Chaos doubling Phenomenon.
- [5] M. Ali, L. M. Saha, Y. Tanaka and Hideo Soga, Non Parametric Periodic orbit as a Singularity of the OGY Stabilisation Technique.
- [6] Robert C. Hillorn, Chaos and Non Linear Dynamics.
- [7] Ali. H. Nayfeh, Balakumar Balachandran, Applied Non Linear Dynamics, Wiley Series in Non Linear Science.
- [8] A. Pikovsky, M. Rosenblum, J. Kurths, Synchronisation : A Universal Concept in Nonlinear Sciences, (Cambridge University Press, 2001).
- [9] A. Y. Loskutov, S. D. Rybalko, U. Feudel, J. Kurths, J. Phys. A 29, 5759–5771 (1996).
- [10] S. Codreanu, A. Savici, Chaos Solitons and Fractals-12, 845–850 (2001).
- [11] Vinod Patidar, K. K. Sud, Synchronising identical chaotic systems using external chaotic driving, Proceedings NCNSD 2005.

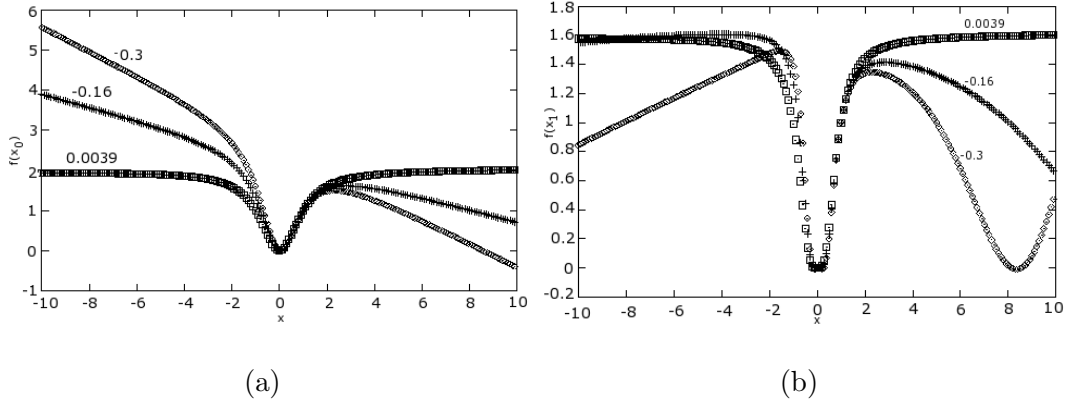


Fig. 1. Variation of a) the function  $f(x)$  b) its first iterate for three different values of  $\mu$   $-0.3$ ,  $-0.16$  and  $0.0039$

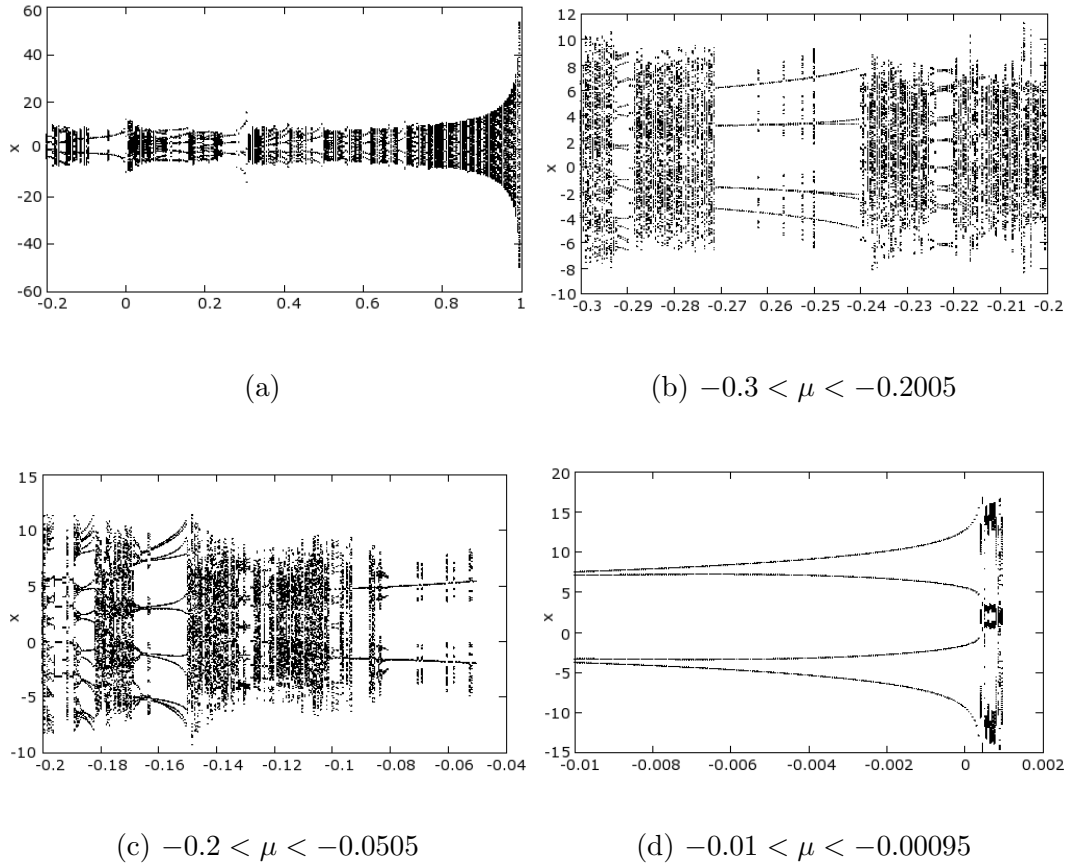
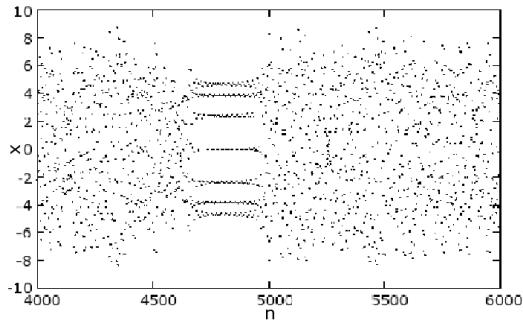
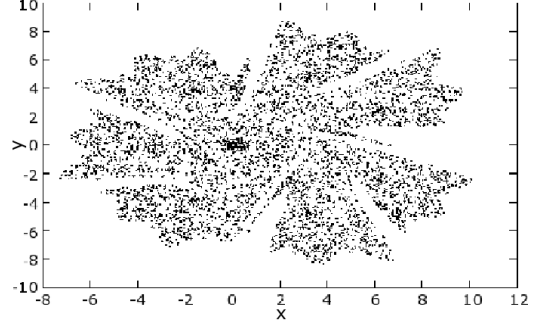


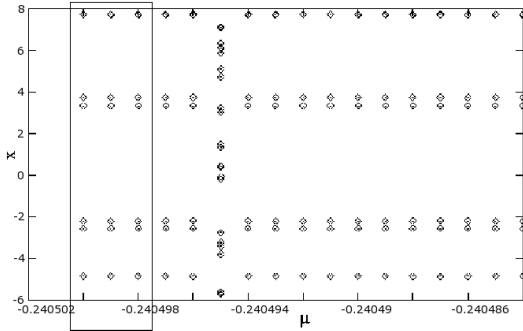
Fig. 2. a) Bifurcation scenario in the range  $\mu = -0.2$  to  $+1$ , for  $a = 0.008$ ,  $b = 0.05$ . The windows of periodic cycles are zoomed for details in b, c and d as indicated.



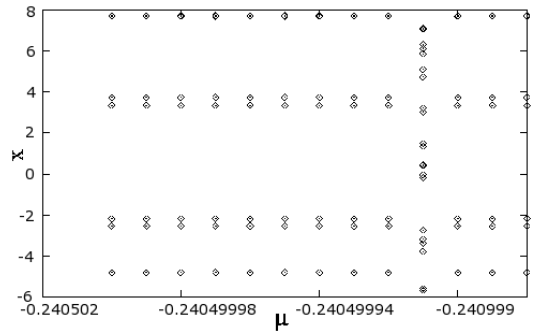
(a)



(b)



(c)



(d)

Fig. 3. The intermittency behaviour before the stabilisation of a 7 cycle is shown in the  $x_n$ - $n$  plot in (a) and corresponding phase portrait in (b) for  $\mu = -0.2734$ . Note that this is the typical behaviour near the onset of each periodic window. The self similar and repeating substructures inside this stability window is shown in Figs 3c and 3d where the 7 and 22 cycles are seen to recur. (The rectangle shown in 3c is zoomed in 3d).

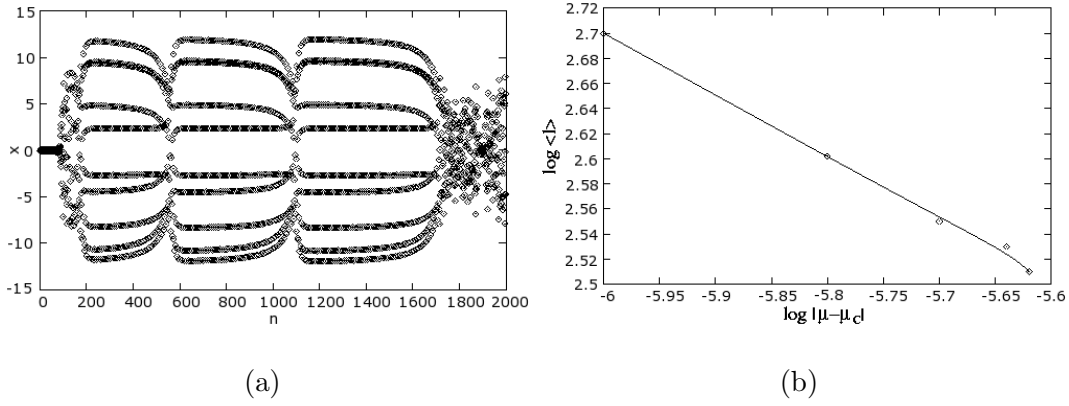


Fig. 4. Type I intermittency near the onset of a 10 cycle a) the laminar and irregular behaviour for  $\mu = -0.312501$  b) the scaling of average laminar region  $\langle l \rangle$  as function of  $|\mu - \mu_c|$  where  $\mu_c = -0.312498$ . The scaling index in this case is  $-0.49$ .

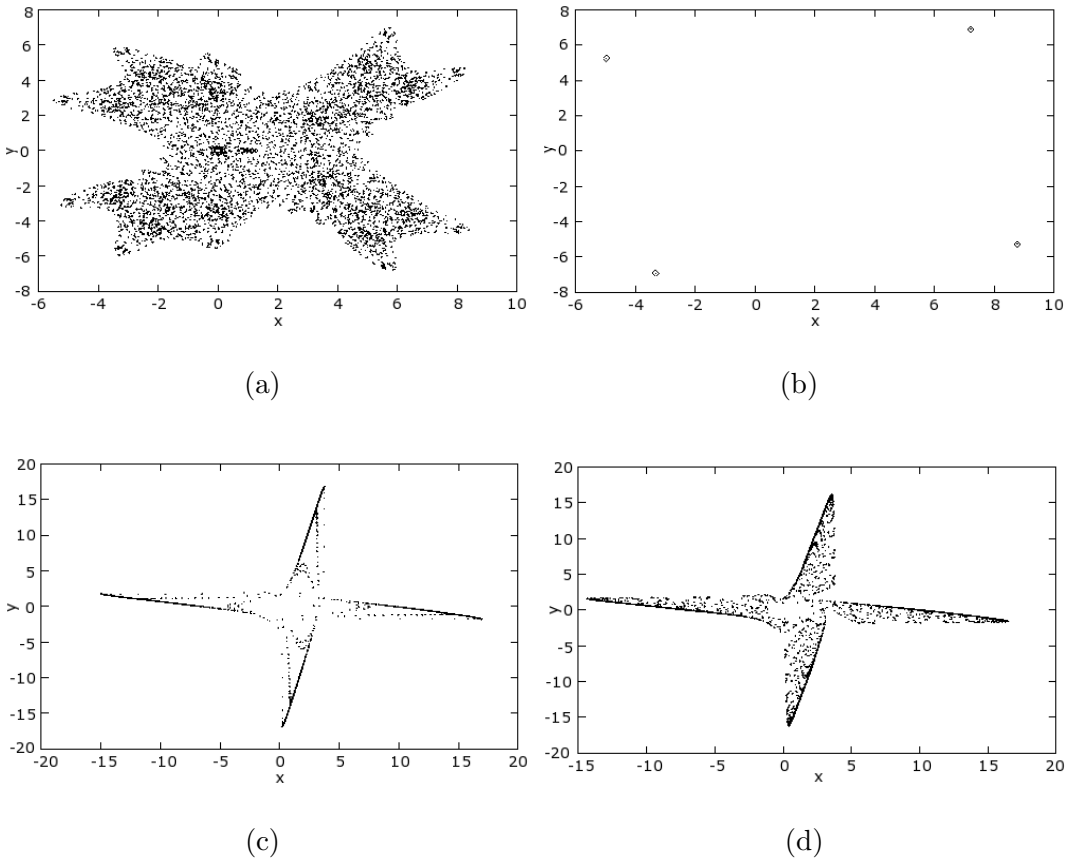
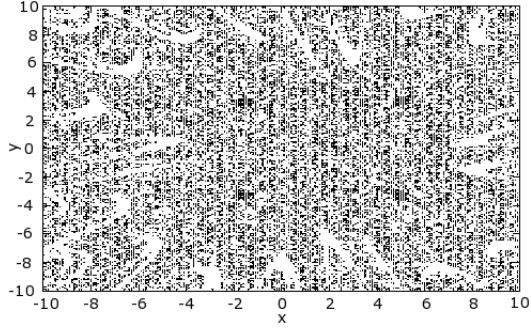
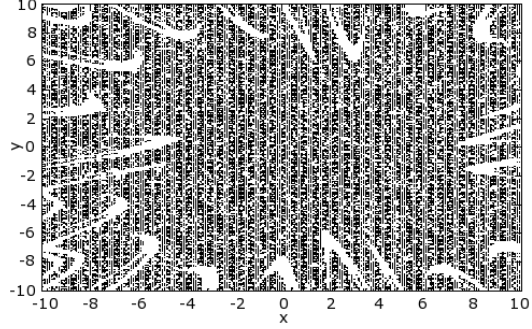


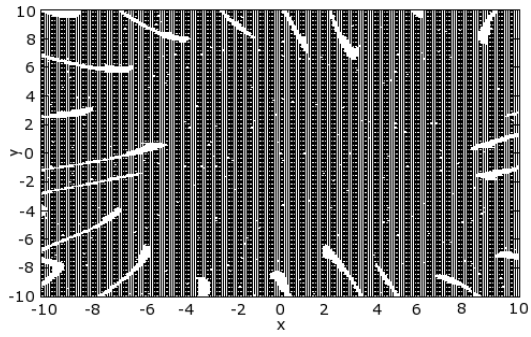
Fig. 5. The phase portraits for  $\mu$  values in the region of the 4 cycle window a) intermittency region ( $\mu = -0.1199$ ) b) stable 4 cycle ( $\mu = -0.005$ ) c) quasiperiodic 4 lands ( $\mu = 0.0003695$ ) and d) chaotic attractor ( $\mu = 0.001$ )



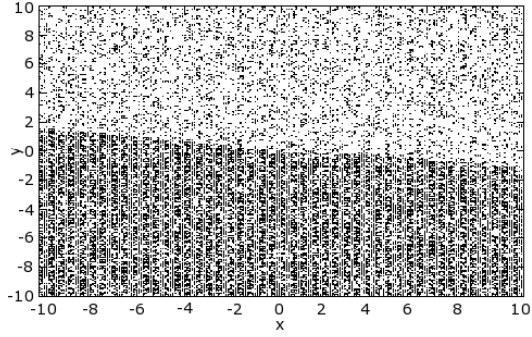
(a)



(b)

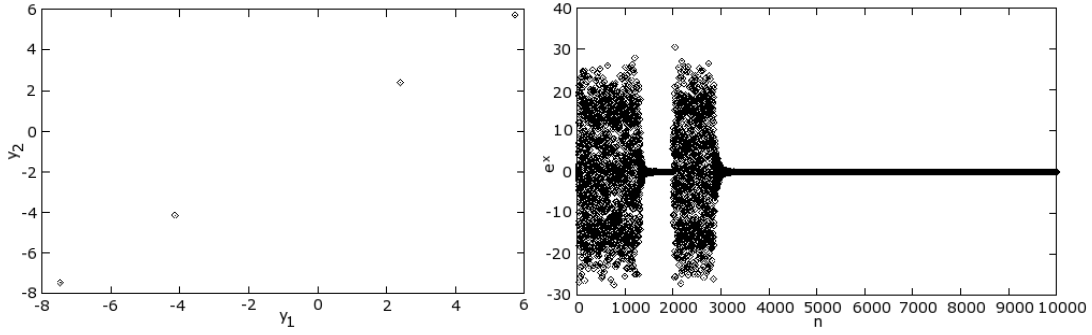


(c)



(d)

Fig. 6. The basin of attraction for the different dynamical states inside the 4 cycle window. Here black region corresponds to the basins of the stable 4 cycle as the  $\mu$  value increases from intermittency towards periodic cycle. a)  $\mu = -0.0815$  b)  $\mu = -0.081$  c)  $\mu = -0.08$ . In (d), the black region corresponds to bounded chaos while white region that of escape for  $\mu = 1.01$ .



(a) The synchronised 4 cycle of two coupled GM maps with linear and mutual coupling for coupling parameter  $\varepsilon = 0.7$ , in eqn. (5).

(b) The synchronisation time  $\tau_1$  and the stabilisation time after perturbation  $\tau_2$  are shown in the  $e^x - n$  plot of the coupled system

Fig. 7.